

Preparation and Characterization of ceramic - metal Functionally Graded Materials for Hip Joint Implants

Alaa Abdulhasan Atiyah¹, and Noor S. Ghafil²

¹ Department of Materials Engineering, University of Technology

Baghdad, Iraq, 130035@uotechnology.edu.iq

² Department of refrigeration & Air Conditioning Techniques Engineering, Dijlah University College

Baghdad, Iraq, noor.aljobory@duc.edu.iq

Abstract

The present study included preparation and characterization of step-wise functionally graded materials (FGMs) for hip joint replacements, prepared by using powder technology technique. ceramic – metal FGMs specimens (AZT Group) that made from nano Al_2O_3 , nano 3YPS-ZrO₂ and Ti – alloy (Ti-6Al-4V), consist of 10 layers begins with 100% Ti – alloy that gradually decreases and Al_2O_3 and 3YPS-ZrO₂ increases, finally ends by 100 % Al_2O_3 . Physical tests for AZT – Group were done in order to characterize FGMs prepared, which includes apparent density & porosity for green compact and for sintered compacts also relative apparent density percentage, all physical tests showed increase in apparent and relative apparent density percentage after sintering process in a range (93-98)% and decrease in porosity (25- 35)% as a range also after sintering process, which it's a great evident that the time and temp. of sintering process chose carefully and gave optimum properties of FGMs specimens. Mechanical tests such as Vickers microhardness, fracture toughness and residual stresses used to characterize prepared of FGMs. All mechanical tests are presented a gradient in results through the cross – section of FGMs specimens as expected from the gradient of composition that shows a smooth transition from layer to another that eliminate the sharp transition. X-rays diffraction was done to investigate phases appears and SEM and EDS analysis also were done for AZT1, which shows higher properties among their groups, display good distributed of 3YPS – ZrO₂ from EDS analytic and there were no agglomerates, which its good evidence of good mixing process and sintering practice.

Key words: Alumina, 3YPS-zirconia, Ti-6Al-4V, hip joints.

1.Introduction

Biomaterials maybe defined biocompatible materials, which be inserted inside the body of human in biological medium in various shapes so as to heal damages of organ and tissue. They also fulfill their functions in the surgery of replacement. Biomaterials with various functions are used to obtain the principal target of refining the life of human. It could easily see in history which the modern civilizations used, for example

seashell and gold that used in replacements of lost tooth in human [1].

Functionally graded materials(FGMs) are composite materials changing their micro-structures from one substance to another in a specific grade, which results analogous varies in the effective characteristics of material (containing modulus of elasticity, modulus of shear and density) for this material. The FGMs can be

prepared to manufacture an optimal distribution for a component with specific purposes, applications and functions [2].

Titanium and its alloys are most widely used for dental and orthopedic implants, due to their high specific strength, superior biocompatibility, high corrosion resistance and elastic modulus which are closer to natural human bones [3].

Recently, Ti-6Al-4V alloys have secured a special place in the bone and joint replacements industry. The alloy confers excellent corrosion resistance to deal with the mechanical load, chemically stable and substrate biocompatibility with relatively low elastic modulus [4].

Bioceramic materials are mainly used as bone tissue replacement. To fulfil this function satisfactorily, they should meet the biocompatibility conditions with live tissue and not display any cytotoxic behaviour. The ceramic materials' biocompatibility is heavily dependent on their chemical composition. However, there are also other properties that affect their biocompatibility, such as phase composition, surface roughness, ceramic materials, or pore size and distribution [5]. Alumina oxide (Al_2O_3) belongs to materials group of oxide ceramic that includes sintered and pure metal oxide. Alumina or aluminium oxide is the noblest

2. Experimental procedure

Ceramic – metal FGM specimens who differentiated in compositions have grouped AZT1, AZT2, AZT3 and AZT4; figure 1 shows is schematic diagram indicates dimensions and compositions of each layers of ceramic – metal FGM. Each ceramic - metal FGM specimen consists of ten compacted layers consisting of alumina, zirconia and titanium alloy (Ti – 6Al – 4V), it can see easily from figure 1 that smooth transition in composition in order to eliminate the effect of different thermal expansion between metal and ceramic many tests is done and finally the successful

oxide. In comparison with metals, Al_2O_3 exhibits an obviously greater compressive strengths & a lesser tensile strength. “Bioloxflexural strength” is roughly similar as “Ti-6Al-4V” & somewhat minor than that of ferrous metals [6]. Zirconia is utilised as a bio-material. It has benefits over other ceramics due to its high physical strength and fracture toughness. Biomaterials have been recommended as artificial bone fillers for restoring bone defects. Zirconia also serves other clinical purposes such as: dental crowns and arthroplasty. Zirconia and yttria stabilised zirconia have orthopaedic uses such as knee and hip prostheses, hip joint heads, tibial plates, temporary supports, and dental crowns [7].

Zirconia (ZrO_2 , zirconium dioxide), also known as “ceramic steel”, has optimal properties for dental application: excellent toughness, strength, and resistance to fatigue, in addition to superior wear qualities and biocompatibility. Zirconium (Zr) is an extremely strong metal with physical and chemical properties similar to titanium (Ti). As a matter of fact, Zr and Ti are two metals generally used in implant dentistry, chiefly because they do not hamper the bone forming cells (osteoblasts), which are necessary for Osseo integration [8].

composition was adopted. Nano alpha – alumina and 3% Y_2O_3 – tetragonal zirconia poly crystals from ssnano company, USA. Ti-alloy (Ti-6Al-4V), titanium from strem, aluminum from CDH and vanadium from ssnano company, more details show in table 1. Powder technology technique was used to prepare FGM specimens, firstly: mixed powders of each layer by ball mill for 60 min. secondly: pressed the powders (10 layers) in stainless steel mold under 150 MPa for 180 sec. for all specimens, AZT1 specimen has composition alumina with max. addition of zirconia 10% and Ti -

alloy, while AZT2 specimen has composition alumina with max. addition of zirconia 20% and Ti - alloy. AZT3 specimen has composition alumina with higher

zirconia percentage 30% and Ti – alloy, AZT4 has composition of alumina with highest percentage of zirconia 40% and Ti –alloy.

Table 1: Materials used in preparing specimens.

Materials powder	Average particle size	Purity	Source
Alumina	50nm	99.9%	ssnano
3Y- Zirconia	25nm	99.9%	ssnano
Titanium	325 μ m	99%	strem
Aluminum	250 μ m	99.8%	CDH
Vanadium	325 μ m	99.5%	ssnano

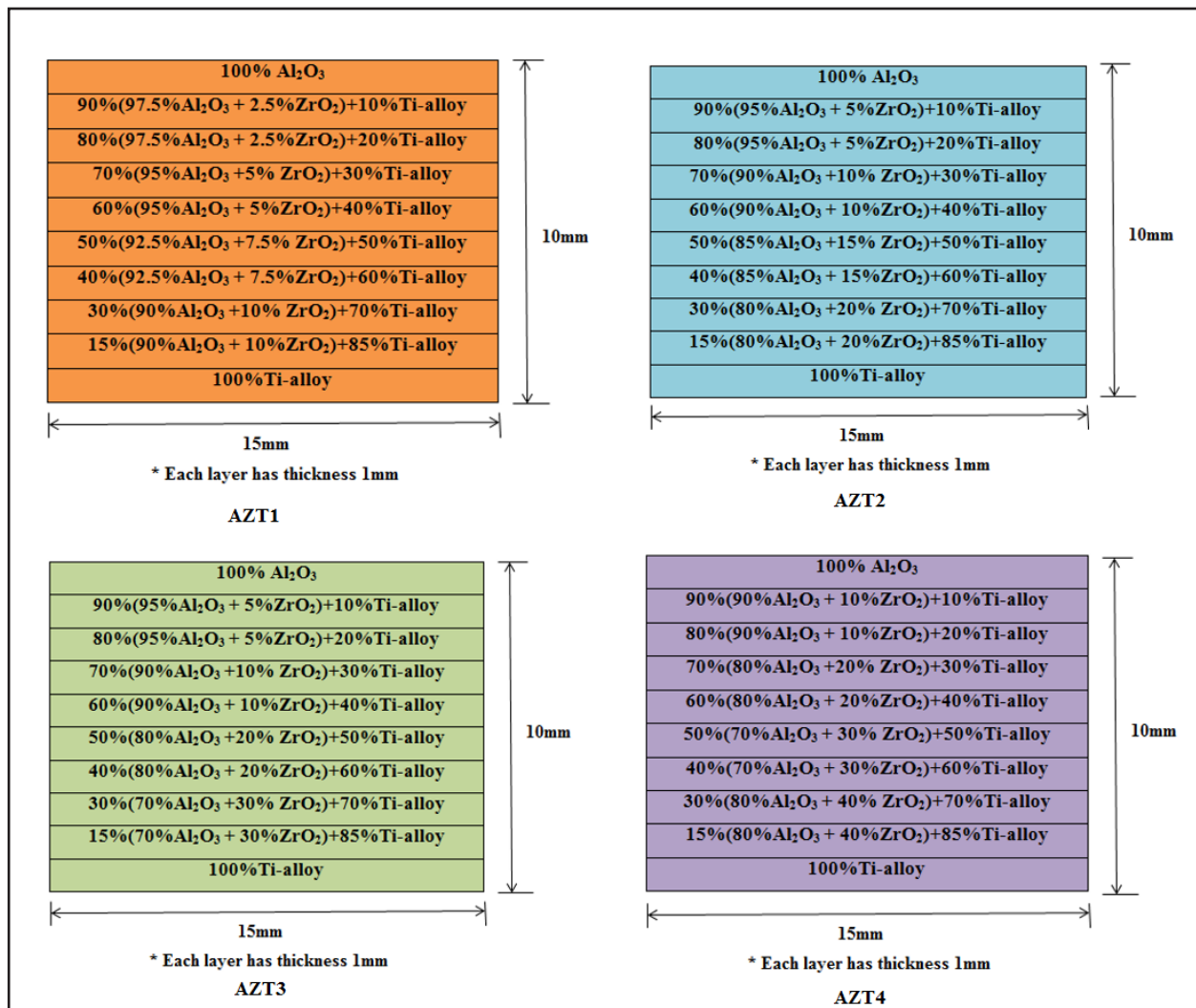


Figure 1: Schematic diagram for dimensions and composition of AZT1, AZT2, AZT3 and AZT4.

Sintering process for AZT- group was done inert gas (argon gas) to prevent oxidation, by heating the specimens to 1250°C at rate 5°C/min. and for 2 hr as dwell time, finally the cycle cools down to room temp. with rate 5°C/min. and figure 2 is presented documents the full furnace cycle.

“Density and porosity” for green and sintered compacts were calculated by

measuring dimensions and weighing of compact specimen after and before sintering practice, dimensional change also calculated after sintering [9]. The relative density for sintered specimens was calculated in ethanol according to the Archimedes principle, assuming the alumina theoretical density is 4.1 gm/cm³ and the 3Y – ZrO₂ theoretical density is 6.05 gm/cm³ [10].

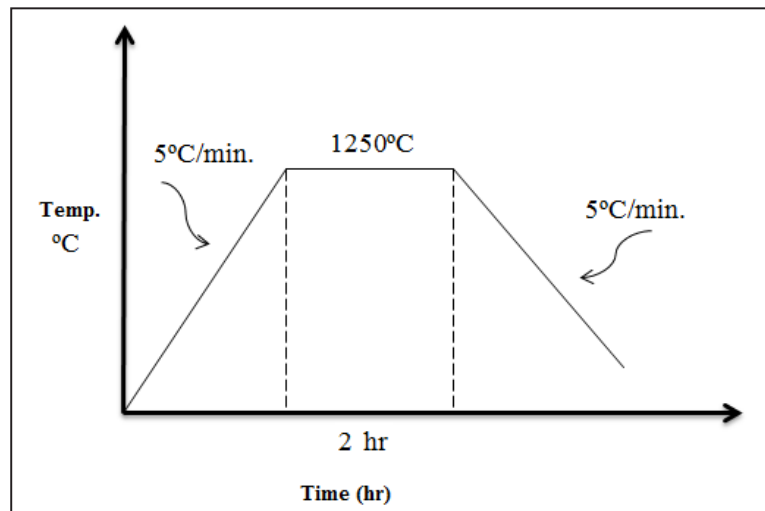


Figure 2:Schematic diagram of sintering process for specimens of AZT Group.

Vickers microhardness is characterized using TH-175 digital microhardness tester; the load is 9.8 N and holding time is 15 sec. on the specimen surface. Fracture toughness was investigated using indentation methods, the indentations were carried out using a standard hardness tester with loading 1 kg.

The indent was aligned thus its diagonals and conceivable radial crack in layers of FGM was perpendicular or parallel. The crack length size was calculated by an optical microscope. Indentation fracture toughness (K_{IC}) is measured by using the Anstis et al. [11] formula:

$$K_{IC} = \eta \sqrt{\left(\frac{E}{H}\right) \frac{P}{c^{3/2}}},$$

Where:” η is a geometric factor predestined (0.016), H is the hardness, E is young’s modulus, P is load of indentation and c is radial crack half – length indentation at the surface”. To calculate E-modulus for FGM

were derived from characteristics of components (Al₂O₃ & 3Y - ZrO₂), lived by the particular volume fraction, according to following formula:

$$E = \frac{E_X \left[E_X + (E_{Al_2O_3} - E_X) V_{Al_2O_3}^{2/3} \right]}{E_X + (E_{Al_2O_3} - E_X) (V_{Al_2O_3}^{2/3} - V_{Al_2O_3})}$$

Where symbol X refers for ZrO₂ composition and “V: is a volumetric fraction”.

Difference in length from cracks (C, unstressed) & perpendicular cracks on the layers (C_R, stressed) and in-plane residual stresses (σ_R) may be determined by [12]:

$$\sigma_R = \frac{K_{IC} - K_I}{Y_{C_R}^{1/2}} = K_{IC} \frac{1 - (c/c_R)^{3/2}}{Y_{C_R}^{1/2}} \quad \begin{array}{l} > 0 \text{ tensile} \\ < 0 \text{ compressive} \end{array}$$

Where:

K_I : is the stress intensity factor for stressed crack.

Y : is the geometric factor ~ 1.26 .

X-ray diffraction (XRD) test for phase identification achieved by using apparatus of Shimadzu (XRD - 6000, Germany), by Cu K α radiation, from 20 – 70 of 2 θ , 40 KV, 30 mA, with step size 0.05 deg. for 0.60 sec. Scanning Electron Microscopy (SEM) - (Tescan Vega-SB) model made in Belgium

is used for inspecting the surface and fracture surface morphology of specimens. To attain a good electric conductivity, all specimens are gold sputtered at surface beside the edge. Then, secondary electron images are recorded, with working voltage is kept at (10 KV).

3. Results and Discussion

3.1 Physical Characterization

The initial ideas of this research was to prepare a continuous high order (10 layers) FGMs. Starting with materials powders (Alumina, zirconia & Ti- alloy), blending powders, application of each layer carefully, compacting & then sintering. Compaction is a great scientific and practical importance; the main issue is to obtain efficient packing. specimens with alumina, zirconia with 3% Y₂O₃ and Ti -alloy (Ti-6 Al-4V alloy) i.e.(AZT1, AZT2, AZT3 and AZT4) shows

results for green density with alumina and zirconia with 3% Y₂O₃, that all FGM compacts possess green density range between originals ingredients densities which is an evidence of good blending and mixing process. Figure 3 shows green density for AZT1, AZT2, AZT3 and AZT4 specimens. Figure 4 shows green porosity for the same specimens and as is evident that the green porosity decreased slightly with increased zirconia content.

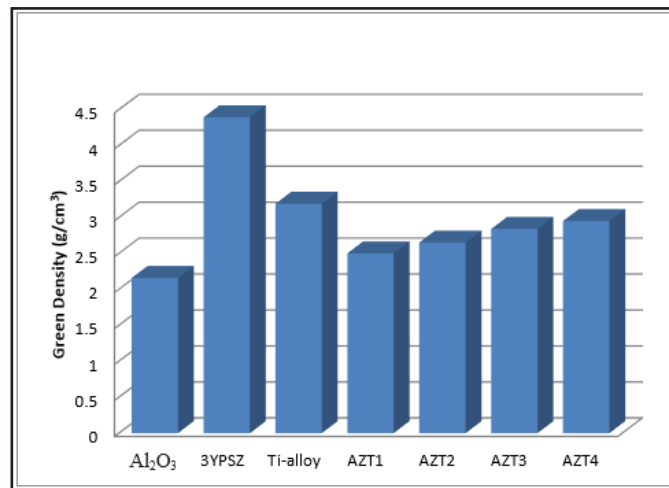


Figure 3: Green density of FGMs specimens as a function of chemical composition.

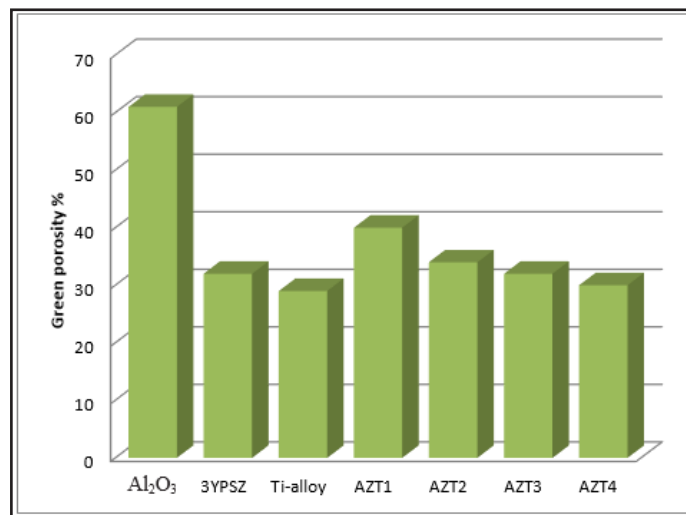


Figure 4: Green porosity of FGMs specimens as a function of chemical composition.

The formation of the density graded from outside of the specimen to inside of the specimen through sintering practice, appears four mechanisms at least as following: firstly, the exothermic reactions together with the atmosphere of the sintering process, where faster densification happens in hottest regions. Secondly, the gradient of the green density, which means density gradient existing before sintering process. Thirdly, the thermal gradient because of fast heating. Fourthly, the development of the coarsening for the gas through sintering process while coarsening here is denote to grains or/and

pores growth without the simultaneous densification [13].

Figure 5 showed apparent density calculated by geometric method. It is obviously that the apparent density increased highly by sintering and porosity decreased, figure 6, but not as is expected due to presence macro cracks found in these specimens. The reasons behind such improvement were the enhancing of diffusion phenomenon by temperature in sufficient time also the density of alumina and Ti – alloy almost same that's lead to good stacking between atoms.

The sintered ceramics and FGM specimens presented a relative density from 93% to 98 %. Broadly, sintered specimens that have higher relative density display greater

mechanical characteristics. Though, it should remember an effect of microstructure homogeneity on mechanical characteristics

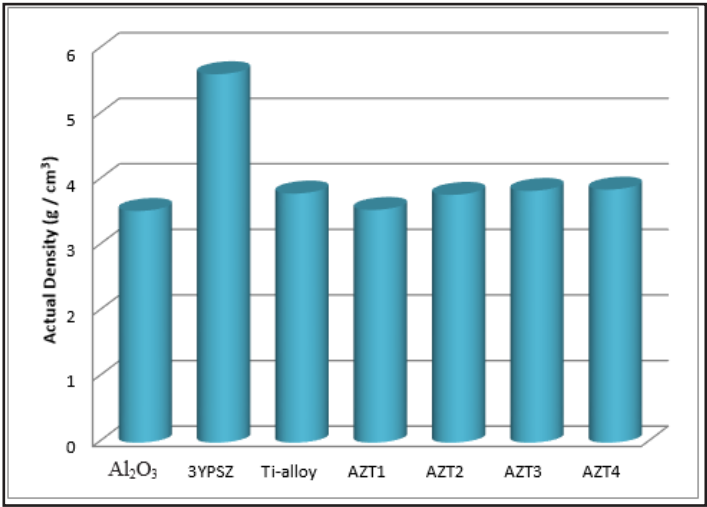


Figure 5: Actual density of ceramic – metal FGMs specimens.

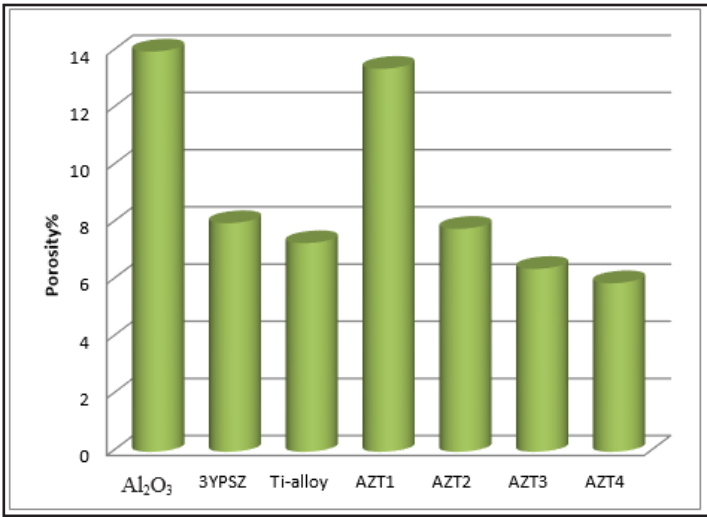


Figure 6: Sintered porosity of ceramic - metal FGMs specimens.

It is clear from this figure 7 that the relative density of specimens ranging among densities of basic components (alumina

zirconia and Ti - alloy) and this great evident that the compaction process and sintering process done successfully.

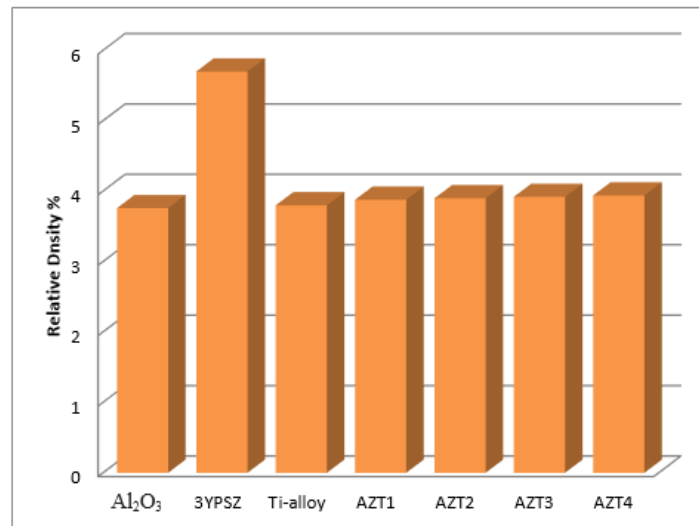


Figure 7: Relative Apparent density% of ceramic – metal FGMs specimens.

Figure 8 shows ceramic –metal specimens, as particles of matrix are sinter among themselves & around the particles of reinforcement that's lead to decrease the porosity especially in the beginning of sintering because nucleation process of particles that loosely packed. As sintering continuous, the consumption of porosity

levels off because of the nonexistence of tiny pores residual to consume as long as the absence of energy to the surface energy of the huge pore sizes that stay. Extra decreases in the porosity may happen because the creation of matrix reduction induced micro stresses, which lead to plastic deformation of the ductile metal phase [14].

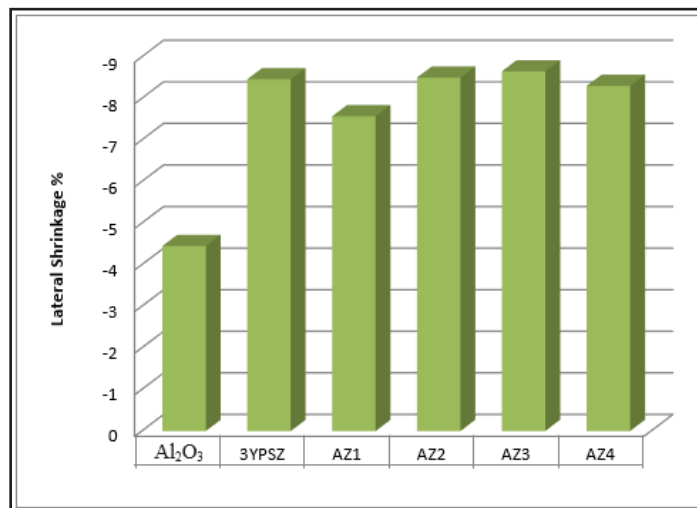


Figure 8: Lateral shrinkage % of ceramic – metal FGMs specimens.

3.2 Vickers Microhardness

The average measured Vickers microhardness is two microhardness measurements were taken on each homogeneous composite layer through the specimens as well as the two faces. The evolution of hardness in a gradient structure is heavily influenced by the residual stresses and shrinkage constraints produced by the compositional gradient. Reducing shrinkage constraints by modifying the sintering

kinetics of the gradient can boost the hardness of the entire specimen.

Figure 9 shows ceramic – metal FGM specimens, it is clear that highest vicker's hardness value is found in the side of pure alumina (1700 kg f/mm³) and decrease towards the other side of Ti – alloy (350 kg f/mm³), the reasons behind the decreasing in hardness values are presence of the soft metal phase and presence of YPS – zirconia (900 kg f/mm³).

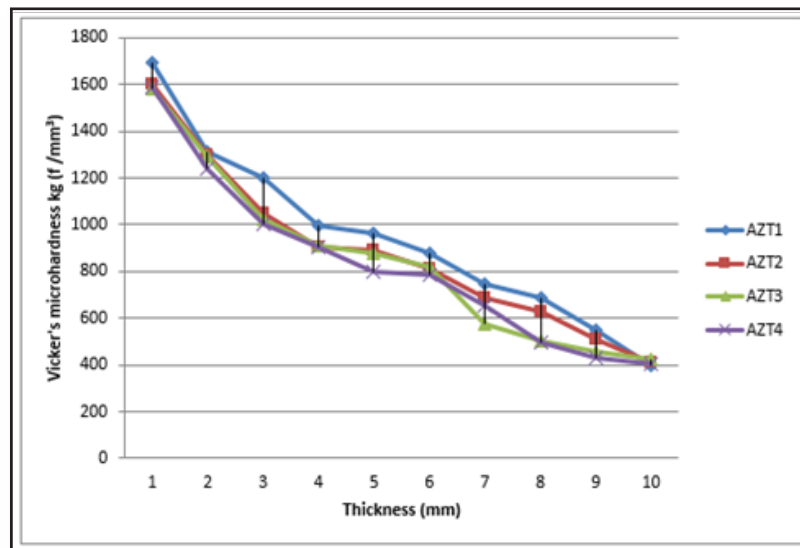


Figure 9: Vicker's microhardness of ceramic - metal FGMs specimens along the thickness.

Figure 10 is presented the fracture toughness of ceramic – metal specimens, as expected the higher fracture toughness in layers that have higher 3YPS-zirconia content, where the tetragonal phase is the toughening agent. As well as, the indent of Vicker's leaves zone with a plastic deformation under it. Producing, a well understanding of the plastic deformation and residual stresses conditions encouraged by indentation in ZTA ceramic, which can support to explore the influence for phase transformation of ZrO₂ on the plastic deformation of the Al₂O₃

matrix and distribution of stresses field after the indentation experiment [15].

Residual stresses (compressive or tension) in the multiphase components are established because of the incompatibility in the modulus of elasticity and “coefficient of thermal expansion (CTE)” amongst constituent phases. However, because of lower CTE of Al₂O₃ ($\alpha = 6.6 \times 10^{-6} \text{ K}^{-1}$) compared to 3YPS- ZrO₂ ($\alpha = 11 \times 10^{-6} \text{ K}^{-1}$) and Ti – alloy is ($\alpha = 9.5 \times 10^{-6} \text{ K}^{-1}$), while the E equal to 380 GPa, 210 GPa, 110 GPa is used for Al₂O₃, 3YPS - ZrO₂, and Ti – alloy respectively [16].

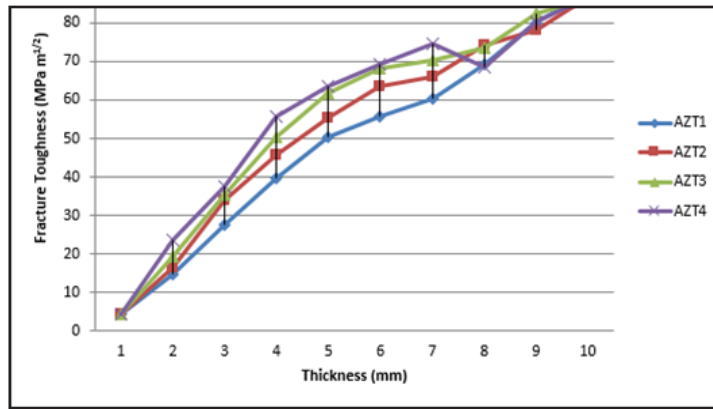


Figure 10: Fracture toughness of ceramic - metal FGMs specimens along the thickness.

Figure 11 is presented the residual stress measurements by indentation of ceramic – metal (AZT) FGMs specimens, it is expected that ceramic – metal specimens is subjected to residual stresses due to mismatch of E – modulus and thermal expansion among constituents during

cooling from sintering temperature. The E–modulus and the CTE of Ti –alloy, which is approximately similar for YPS- zirconia and higher than alumina and this lead to produce compressive stresses in alumina pure layer and rich alumina content layers and tensile stresses in layers rich Ti – alloy.

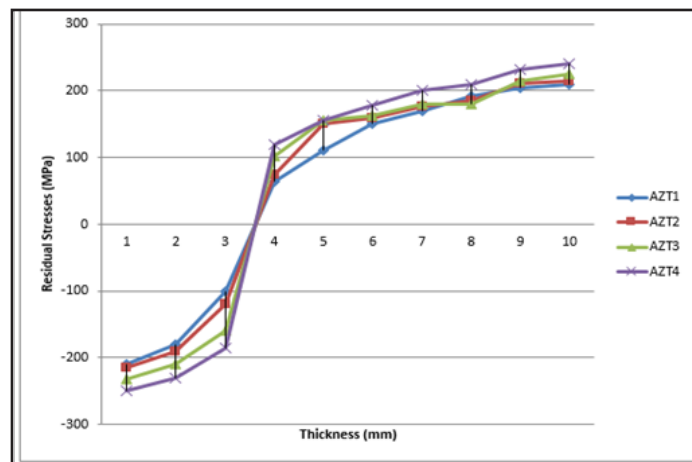


Figure 11: Residual stresses of ceramic - metal FGMs specimens along the thickness.

3.3 X-Rays Diffraction

Figure 12 is show Ti – alloy after sintering, which the main phase is α (Ti) phase found during the X- rays diffraction analysis

although some β (Ti) phase and Al₂V₃ phase were detected, this indicating that the composition of Ti – alloy is not

homogeneous. The presence of β (Ti) phase peak indicates that alloying elements were already dissolved in the Ti matrix, which stabilizing the β (Ti) phase [17].

X- rays diff. test was done along the cross section (along 10 layers) to investigate

phases appeared after sintering, all specimens contains α – alumina, 3YPS – zirconia (tetragonal phase) and α (Ti) phase, β (Ti) phase and Al₂V₃ phase were detected, figure 13 is presented X – rays pattern for AZT1 specimen.

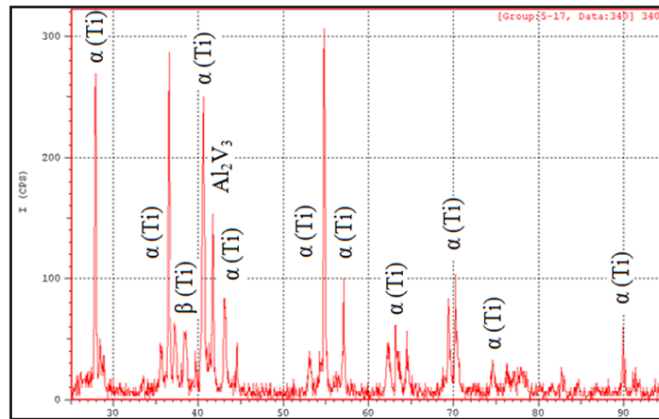


Figure 12: X-rays diffraction pattern for Ti –alloy (Ti – 6Al – 4V).

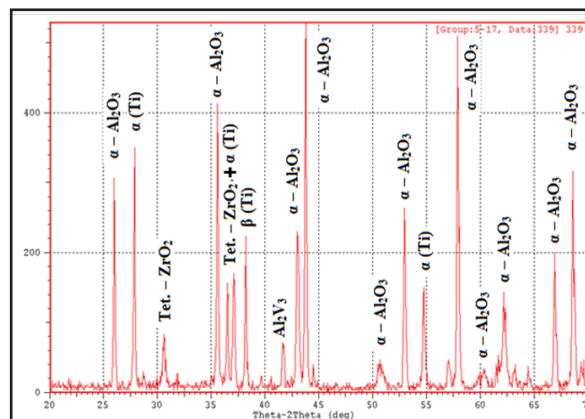


Figure 13: X-rays diffraction pattern for AZT1 specimen along cross - section.

3.4 Microstructure Observations

Figure 14 is presented EDS analytic and SEM for AZT1 ceramic – metal FGM specimen, which contains 10% of 3YPS- ZrO₂, for five locations along the cross section of AZT1 from ceramic side. The AZT1/1 which is rich with alumina, Al & O are the domain elements. Ti increased gradually along AZT1 with decreased in Al & O, no detections of Zr, Y and V and appearance of Ca&Cl as impurities. Also its

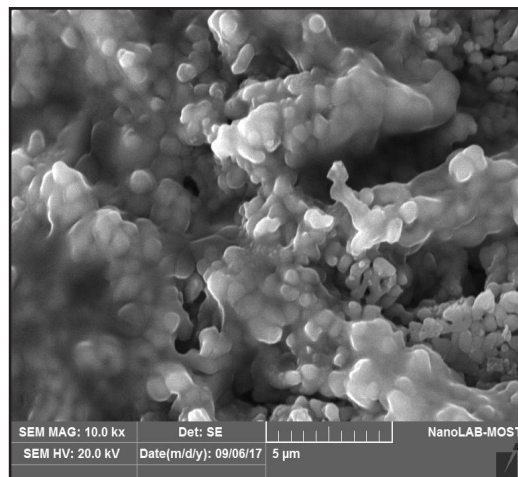
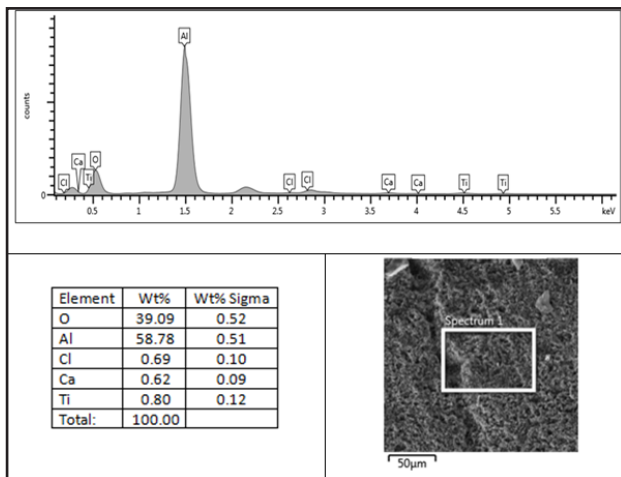
shown from figure 14 five images of SEM that AZT1/1 has only alumina & zirconia only, good compaction in the first layer while AZT1/5 has only Ti – alloy. As proceed towards other layers it can see that increasing with Ti - alloy the porosity decreasing due to the high plasticity of metal phase that fills vacancies and there were no porosity that results from binder removal.

Position

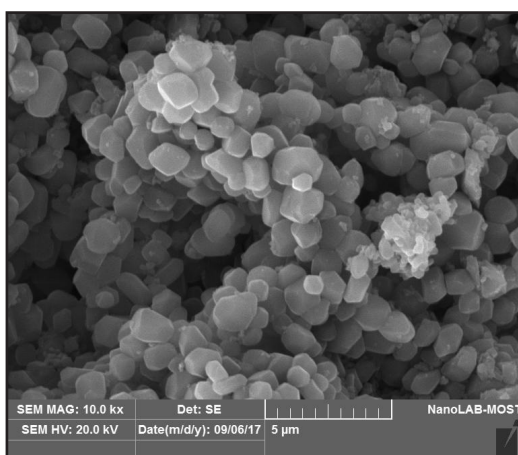
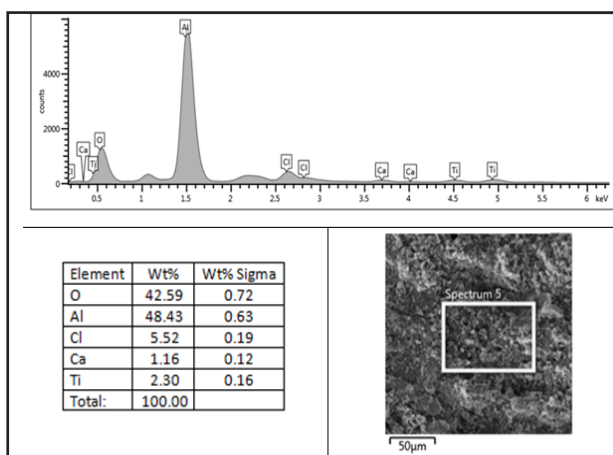
EDS

Magnification X 10K

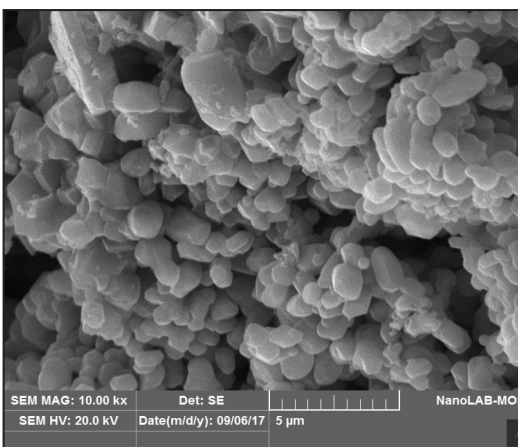
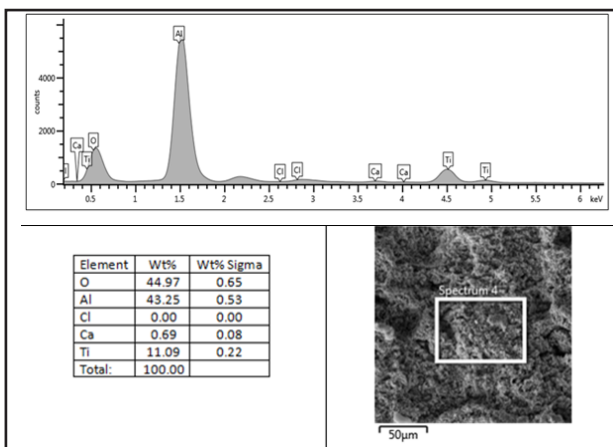
AZT1/1



AZT1/2



AZT1/3



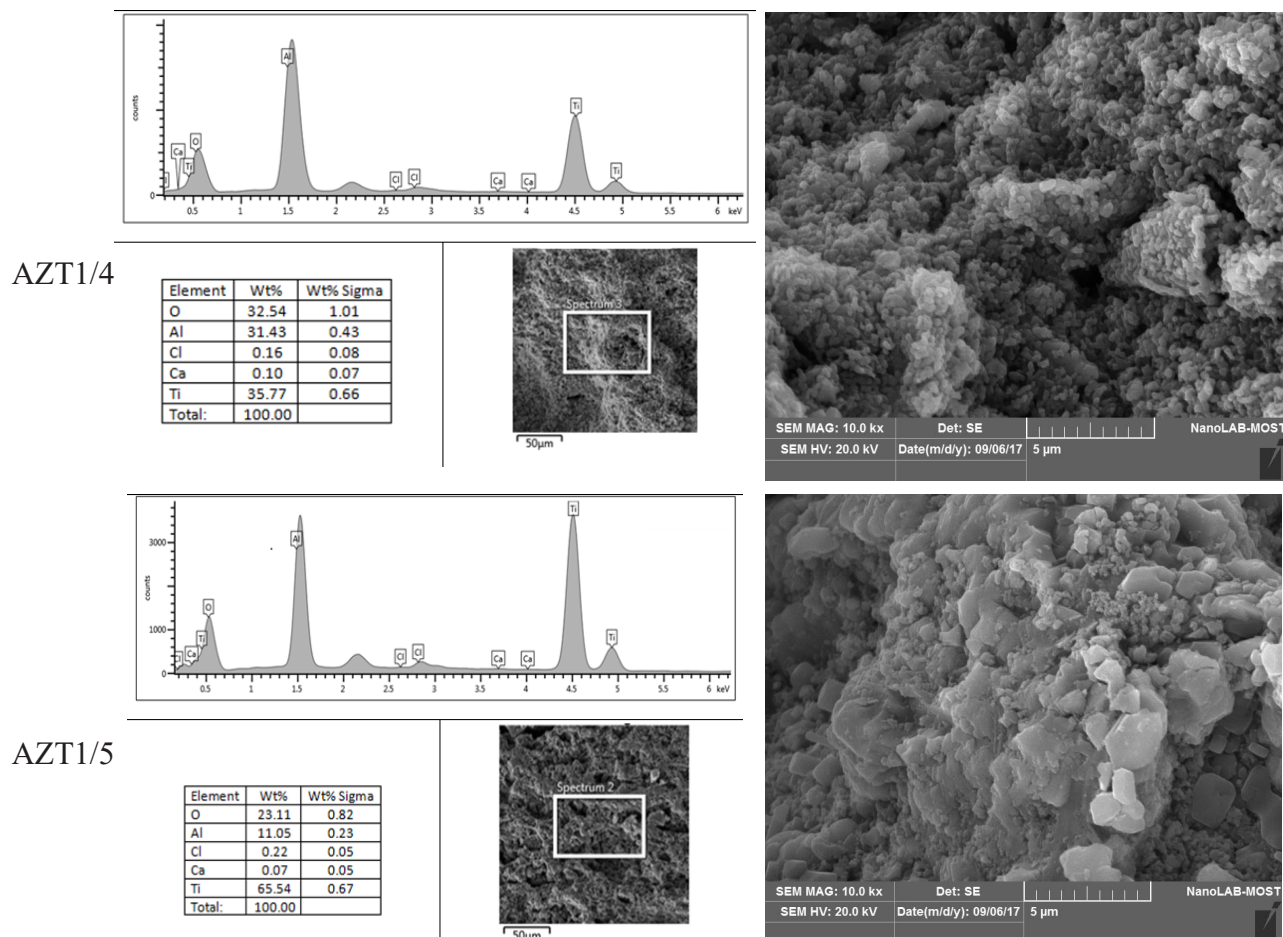


Figure 14:SEM observation for ceramic – metal AZT1 FGMs specimens.

4. Conclusion

High order FGMs prepared successfully from nano alumina, nano 3YPS-zirconia and Ti -alloy good packing in all layers, higher apparent density and lower porosity than individual constituents. Higher hardness

5. References

1. Bandyopadhyay, “Characterization of Biomaterials”, School of Mechanical and Materials Engineering Washington State University Pullman, WA, USA, Elsevier, 2013.
2. L. Li, Y. Hu, “Nonlinear bending and free vibration analyses of nonlocal strain gradient beams made of functionally graded material”, International Journal

of Engineering Science, Vol. 107, pp.(77–97), 2016.

3. S. Sathish, M. Geethaa, S.T. Aruna, N. Balaji, K.S. Rajam, R. Asokamania, “Sliding wear behavior of plasma sprayed nanoceramic coatings for biomedical applications”, Wear, vol. 271, pp. (934– 941), 2011.

of Engineering Science, Vol. 107, pp.(77–97), 2016.

3. S. Sathish, M. Geethaa, S.T. Aruna, N. Balaji, K.S. Rajam, R. Asokamania, “Sliding wear behavior of plasma sprayed nanoceramic coatings for biomedical applications”, Wear, vol. 271, pp. (934– 941), 2011.

4. J. CIZEK, “Thermally Sprayed Bio-Ceramic Coatings: A Study On Process

Parameters Influence On Coating Properties”, School Of Mechanical And Aerospace Engineering, Nanyang Technological University, 2010.

5. A. Matoušek, M. Kukletová and J. Cihlář, “Influence of nanograin size of ZrO₂ and Al₂O₃ ceramics on biological response of cells”, Key Engineering Materials, Trans Tech Publications, Switzerland, Vol. 587, pp.(132-137), 2013.

6. J. M. Kruszynski, “Comparative Study of Alumina and Tetragonal zirconia Composite Ceramics for Structural Applications”, Ph. D. thesis, Science and Technology of Materials and Sensors, 2008.

7. A. D. Bona, O. E. Pecho and R. Alessandretti, “Zirconia as a Dental Biomaterial”, Materials, Vol. 8, pp. (4978-4991), 2015.

8. B. AL-AMLEH, K. LYONS & M. SWAIN, “Clinical trials in zirconia: a systematic review”, Journal of Oral Rehabilitation, Vol. 37, pp. (641–652), 2010.

9. N. SH. Ghfil, “preparation and characterization of step-wise Cu/Ni functionally graded materials”, MSc, thesis, materials engineering department, university of Technology, 2011.

10. D. Yang, H. Conrad, “Enhanced sintering rate and finer grain size in yttria-stabilized zirconia (3Y-TZP) with combined DC electric field and increased heating rate”, Materials Sci. Eng., Vol. 528(3), pp. (1221–5), 2011.

11. P. Hvizdo, D. Jonsson, M. Anglada, G. Anné, O. Van Der Biest, “Mechanical properties and thermal shock behaviour of alumina/zirconia functionally graded material prepared by electrophoretic deposition”, Journal of the European Ceramic Society, Vol. 27, pp. (1365–1371), 2007.

12. M. Mazaheri, M. Valefi, Z. Razavi-Hesabi, S.K. Sadrnezhaad, “Two-step sintering of nano crystalline 8Y₂O₃ stabilized ZrO₂ synthesized by glycine nitrate process”, Ceramics International, Vol. 35, p. (13–20), 2009.

Parameters Influence On Coating Properties”, School Of Mechanical And Aerospace Engineering, Nanyang Technological University, 2010.

5. A. Matoušek, M. Kukletová and J. Cihlář, “Influence of nanograin size of ZrO₂ and Al₂O₃ ceramics on biological response of cells”, Key Engineering Materials, Trans Tech Publications, Switzerland, Vol. 587, pp.(132-137), 2013.

6. J. M. Kruszynski, “Comparative Study of Alumina and Tetragonal zirconia Composite Ceramics for Structural Applications”, Ph. D. thesis, Science and Technology of Materials and Sensors, 2008.

7. A. D. Bona, O. E. Pecho and R. Alessandretti, “Zirconia as a Dental Biomaterial”, Materials, Vol. 8, pp. (4978-4991), 2015.

8. B. AL-AMLEH, K. LYONS & M. SWAIN, “Clinical trials in zirconia: a systematic review”, Journal of Oral Rehabilitation, Vol. 37, pp. (641–652), 2010.

9. N. SH. Ghfil, “preparation and characterization of step-wise Cu/Ni functionally graded materials”, MSc, thesis, materials engineering department, university of Technology, 2011.

10. D. Yang, H. Conrad, “Enhanced sintering rate and finer grain size in yttria-stabilized zirconia (3Y-TZP) with combined DC electric field and increased heating rate”, Materials Sci. Eng., Vol. 528(3), pp. (1221–5), 2011.

11. P. Hvizdo, D. Jonsson, M. Anglada, G. Anné, O. Van Der Biest, “Mechanical properties and thermal shock behaviour of alumina/zirconia functionally graded material prepared by electrophoretic deposition”, Journal of the European Ceramic Society, Vol. 27, pp. (1365–1371), 2007.

12. M. Mazaheri, M. Valefi, Z. Razavi-Hesabi, S.K. Sadrnezhaad, “Two-step sintering of nano crystalline 8Y₂O₃ stabilized ZrO₂ synthesized by glycine nitrate process”, Ceramics International, Vol. 35, p. (13–20), 2009.